0026-895X/07/7201-141–151$20.00
MOLECULAR PHARMACOLOGY
Vol. 72, No. 1
34009/3215147
Mol Pharmacol 72:141–151, 2007
Printed in U.S.A.

Cholesterol-Like Effects of Selective Cyclooxygenase Inhibitors and Fibrates on Cellular Membranes and Amyloid-β Production[S]

Martin Gamerdinger, Angela B. Clement, and Christian Behl

From the Department of Pathobiochemistry, Medical School, Johannes Gutenberg University, Mainz, Germany

Received January 5, 2007; accepted March 29, 2007

ABSTRACT

Strong evidence suggests a mechanistic link between cholesterol metabolism and the formation of amyloid-β peptides, the principal constituents of senile plaques found in the brains of patients with Alzheimer's disease. Here, we show that several fibrates and diaryl heterocycle cyclooxygenase inhibitors, among them the commonly used drugs fenofibrate and celecoxib, exhibit effects similar to those of cholesterol on cellular membranes and amyloid precursor protein (APP) processing. These drugs have the same effects on membrane rigidity as cholesterol, monitored here by an increase in fluorescence anisotropy. The effect of the drugs on cellular membranes was also reflected in the inhibitory action on the sarco(endo)plasmic reticulum Ca^{2+}-ATPase, which is known to be inhibited by excess ordering of membrane lipids. The drug-induced decrease of membrane fluidity correlated with an increased association of APP and its β-site cleaving enzyme BACE1 with detergent-resistant membranes (DRMs), which represent membrane clusters of substantial rigidity. DRMs are hypothesized to serve as platforms for the amyloidogenic processing of APP. According to this hypothesis, both cholesterol and the examined compounds stimulated the β-secretase cleavage of APP, resulting in a massive increase of secreted amyloid-β peptides. The membrane-ordering potential of the drugs was observed in a cell-free assay, suggesting that the amyloid-β promoting effect was analog to cholesterol due to primary effect on membrane rigidity. Because fenofibrate and celecoxib are widely used in humans as hypolipidemic drugs for prevention of atherosclerosis and as anti-inflammatory drugs against arthritis, possible side effects should be considered upon long-term clinical application.

According to the amyloid cascade hypothesis, the formation of amyloid-β peptides derived from the amyloid precursor protein (APP) is causally associated with the pathogenesis of Alzheimer's disease (AD). This hypothesis is substantiated by several lines of evidence: 1) amyloid-β peptides are found accumulated in extracellular plaques in the brains of patients with AD; 2) several genetic predispositions exist with mutations concerning APP itself or components of the γ-secretase complex (presenilins), one of the APP processing enzymes; 3) increased APP dosage by triplication of APP gene locus in Down syndrome (trisomy 21) or by APP gene locus duplication and promoter mutations that increase APP expression promote the progression of AD; and 4) the toxicity of aggregated amyloid-β peptides is clearly documented in vitro (Hardy and Selkoe, 2002; Rovelet-Lecrux et al., 2006; Theuns et al., 2006). Besides few familial forms with the aforementioned mutations, most cases of AD are age-associated and sporadic; therefore, other factors promoting the formation of amyloid-β peptides over time have to be considered. In this regard, alterations in the lipid metabolism, particularly disturbances of cholesterol homeostasis, may represent high-risk factors (Shobab et al., 2005). Because amyloid-β production accelerates with increasing cholesterol concentrations and vice versa, cholesterol is now considered

This work was supported by grants from the Deutsche Alzheimer Stiftung and the Fritz und Hildegard Berg-Stiftung (to C.B.).
Article, publication date, and citation information can be found at http://molpharm.aspetjournals.org.
doi:10.1124/mol.107.034009.
[S] The online version of this article (available at http://molpharm.aspetjournals.org) contains supplemental material.

ABBREVIATIONS: AD, Alzheimer's disease; APP, amyloid precursor protein; BACE1, β-site amyloid precursor protein cleaving enzyme 1; BiP/GRP78, immunoglobulin heavy chain-binding protein/glucose-regulated protein, 78 kDa; APP CTFα/β, α/β-secretase-cleaved amyloid precursor protein C-terminal fragments; DPH, 1,6-diphenyl-1,3,5-hexatriene; DRM, detergent-resistant membranes; ER, endoplasmic reticulum; MBS, 2(*N*-morpholino)-ethanesulfonic acid-buffered saline; PAGE, polyacrylamide gel electrophoresis; PBS, phosphate-buffered saline; sAPPα, α-secretase-cleaved soluble amyloid precursor protein; SERCA, sarco(endo)plasmic reticulum Ca^{2+}-ATPase; COX, cyclooxygenase; CHO, Chinese hamster ovary; DMSO, dimethyl sulfoxide; PCR, polymerase chain reaction; MES, 4-morpholineethanesulfonic acid; CHAPS, 3-[(3-cholamidopropyl)dimethylammonio]-1-propanesulfonic acid; ELISA, enzyme-linked immunosorbent assay; DuP-697, 5-bromo-2-(4-fluorophenyl)-3-(4-(methylsulfonyl)phenyl)-thiophene; SC-560, 5-(4-chlorophenyl)-1-(4-methoxyphenyl)-3-(trifluoromethyl)-1*H*-pyrazole.

to be an important factor involved in the regulation of APP processing.

Cholesterol acts as an essential membrane constituent and drives the otherwise fluid membrane bilayer into a more rigid state. By varying cholesterol concentrations in cellular membranes, cells form different hydrophobic environments, such as the more fluid endoplasmic reticulum (ER) membrane or the more rigid plasma membrane (Maxfield and Tabas, 2005). Cholesterol increases the order in liquid membranes by aligning the long fatty acid acyl chains of phospholipids more perpendicular to the plane of the membrane, which in turn results in a thicker and more rigid membrane. Because alterations of membrane thickness affect conformation of membrane-embedded proteins, the function of several membrane-spanning and membrane-associated enzymes is altered by cholesterol as well (Li et al., 2004; Maxfield and Tabas, 2005).

The amyloidogenesis occurring in AD is strongly associated with cellular membranes, considering that amyloid-β peptides derive from sequential cleavage of the transmembrane amyloid precursor protein by two membrane-bound proteases, the β- and γ-secretase. As a result, APP processing by these enzymes might be affected by the hydrophobic environment and thus directly or indirectly by cholesterol (Lehmann et al., 1997; Lammich et al., 1999; Vassar et al., 1999; Shobab et al., 2005). In particular, the first step in the amyloidogenic cascade exerted by BACE1 may take place exclusively in highly specialized cholesterol-enriched membrane microdomains (Cordy et al., 2003). These membrane domains consist of tightly packed membrane lipids and proteins, which render them resistant to mild detergents. Because integrity of these detergent-resistant membranes (DRMs) depends on the cholesterol content (Pike, 2004), the cleavage of APP by BACE1 consequently correlates with cholesterol concentrations (Simons et al., 1998).

In recent studies, the selective cyclooxygenase-2 (COX-2) inhibitor celecoxib and likewise the peroxisome proliferator-activated receptor-α agonist fenofibrate were reported to alter γ-secretase activity, resulting in enhanced production of amyloid-β 42 (Kukar et al., 2005). Celecoxib shares some similarities in activity with cholesterol in that both exert inhibitory effects on sarco(endo)plasmic Ca^{2+}-ATPases (SERCA) (Johnson et al., 2002; Li et al., 2004). Regarding cholesterol, the lipid-ordering effects on ER membranes are causally implicated with SERCA inhibition. Hence, we hypothesized that celecoxib and fenofibrate provoke lipid-ordering effects in biological membranes similar to cholesterol and that their impact on cellular membranes leads to altered activity of membrane-associated enzymes. Herein, we report that several selective diaryl heterocycle COX inhibitors and fibrates mimic cholesterol effects concerning biological membranes and the function of membrane-spanning proteins, in particular the activity of β- and γ-secretase.

Materials and Methods

Cell Culture and Treatments. Mouse neuroblastoma cell line (N2a) was purchased from the American Type Culture Collection (CCL131; Manassas, VA). Primary human fibroblasts IMR-90 cell line was purchased from Coriell Institute for Medical Research (Camden, NJ). $N2a_{Swe}$ and CHO_{Swe} cells (kind gifts of Drs. C. U. Pietrzik and S. Weggen, respectively) are stably transfected cell lines bearing the "Swedish" mutant variant of human APP_{695} (K595N and M596L) (Mullan et al., 1992). IMR-90 cells were cultured in phenol-red free HEPES-buffered Dulbecco's modified Eagle's medium, N2a, $N2a_{Swe}$, and CHO_{Swe} cells were cultured in a 1:1 mixture of phenol-red free HEPES-buffered Dulbecco's modified Eagle's medium and OPTI-MEM (both from Invitrogen, Karlsruhe, Germany). Media were supplemented with 1 mM sodium pyruvate, 100 U/ml penicillin, 100 U/ml streptomycin (Invitrogen), and 5% (v/v) fetal bovine serum (Invitrogen). When cellular membranes were prepared, a serum with a defined lipid profile (charcoal-dextran-treated fetal bovine serum; HyClone, South Logan, UT) was used to decrease variability caused by lot-to-lot changes of serum. The medium of $N2a_{Swe}$ and CHO_{Swe} cells was additionally supplemented with 200 μg/ml G418 to maintain the selective pressure (Calbiochem, Darmstadt, Germany), but G418 was omitted during all experiments. Cells were maintained at 37°C with 5% CO_2. In all experiments, treatments were performed on nearly confluent cell cultures in 10-cm dishes. Stock solutions of fenofibrate, gemfibrozil, ciprofibrate, bezafibrate (all from Sigma, Taufkirchen, Germany), valdecoxib, DuP-697, clofibrate, SC-560 (all from Cayman Chemical, Ann Arbor, MI), thapsigargin, tunicamycin (Alexis, Lausanne, Switzerland), and celecoxib (LKT Laboratories, St. Paul, MN) were made in 100% DMSO (Sigma). The stock solutions were directly diluted into media immediately before the treatment of cells. In all assays, the concentration of DMSO never exceeded 0.2% (v/v). Cholesterol (Sigma) was added in a complex with methyl-β-cyclodextrin (Sigma). For the cholesterol/methyl-β-cyclodextrin-complex, 500 mg of methyl-β-cyclodextrin were dissolved in 5.5 ml of PBS in a glass tube, warmed to 80°C, and under continuous stirring successively mixed with 25-μl aliquots of 15 mg of cholesterol dissolved in 200 μl of isopropanol/chloroform (2:1). The resulting cholesterol/methyl-β-cyclodextrin complex contained 6.8 mM cholesterol and 70 mM methyl-β-cyclodextrin.

Immunoblot Analysis and Immunoprecipitation. Total protein lysates from subconfluent cell cultures were prepared in a buffer containing 62.5 mM Tris, 1 mM EDTA, 2% (w/v) SDS, and 10% (w/v) sucrose supplemented with 1% (v/v) protease inhibitor mix (Sigma). Total protein (15 μg) was subjected to standard SDS-polyacrylamide gel electrophoresis (PAGE) and transferred to nitrocellulose membranes. Incubation of membranes with primary antibody, diluted in PBS, 0.05% Tween 20, was carried out overnight at 4°C. Then, membranes were incubated with horseradish peroxidase-conjugated secondary antibodies (Jackson ImmunoResearch Laboratories Inc., West Grove, PA) for 1.5 h. Membrane-bound secondary antibodies were detected using the Super Signal Enhanced Chemiluminescence procedure (Pierce, Rockford, IL) and visualized with the Fuji LAS-3000 intelligent dark box (Fujifilm, Dusseldorf, Germany). The following antibodies were used throughout this study: polyclonal anti-APP C-terminal antibody (A8717, 1:1000; Sigma), monoclonal anti-human amyloid-β (1–17)-specific antibody (clone 6E10, 1:1000; BioCat, Heidelberg, Germany), polyclonal anti-BACE antibody (Ab-2, 1:1000; Oncogene/Calbiochem, Darmstadt, Germany), monoclonal anti-Flotillin1 antibody (clone 18, 1:250; BD Biosciences, Heidelberg, Germany), monoclonal anti-BiP/GRP78 antibody (clone 40, 1:1000; BD Biosciences), and anti-α-tubulin monoclonal antibody (clone: DM1A, 1:1000; Sigma).

For detection and quantification of secreted amyloid-β peptides, media from $N2a_{Swe}$ cells treated for 18 h with various agents were harvested, supplemented with 1% (v/v) protease inhibitor mix (Sigma), cleared of cell debris, and then immunoprecipitated with the monoclonal human amyloid-β (1–17)-specific antibody 6E10 (2 μg/ml) using protein G Sepharose (GE Healthcare, Munich, Germany). Medium input used in the immunoprecipitation was normalized to the protein amount of the corresponding cell extracts. Immunocomplexes were washed three times with washing buffer (150 mM NaCl, 50 mM Tris, 1% Nonidet P-40, and 0.02% NaN_3) and heated for 5 min at 99°C in SDS-PAGE loading buffer (10% SDS, 20% glycerine, 125 mM Tris, 1 mM EDTA, 0.002% bromphenol blue, and 10% β-mercaptoethanol). Then immunoprecipitated proteins were

separated by SDS-PAGE and subjected to immunoblot analysis using 6E10 antibody.

Real-Time Reverse Transcription-PCR Analysis. Relative quantification of mRNA levels was performed as described previously (Gamerdinger et al., 2006). In brief, total RNA from subconfluent cell cultures was extracted using the NucleoSpin RNA II Kit according to the manufacturer's instructions (Macherey-Nagel, Dueren, Germany). Reverse transcription was performed on 1 μg of total RNA using the Omniscript Reverse Transcription Kit (QIAGEN, Hilden, Germany) and 1 μM oligo(dT)23 primer (Sigma). Synthesis of cDNA was carried out for 60 min at 37°C. Real-time PCR was performed in a 25-μl reaction volume containing 1 μl of cDNA, 0.5 μl of sense and antisense primers (100 pmol; MWG-Biotech AG, Ebersberg, Germany), and 12.5 μl of 2× Absolute QPCR SYBR Green Mix (ABgene, Epsom, UK) using the iCycler real-time thermocycler (Bio-Rad Laboratories, Hercules, CA). The PCR cycle number that generated the first fluorescence signal above threshold (C_T) was determined. The generation of specific PCR products was confirmed by melting-curve analysis. The relative expression ratio R of target genes was calculated using the relative expression software tool (Pfaffl et al., 2002). Primer pair used to amplify mouse BACE1 was 5′-CAGTGGGACCACCAACCTTC-3′ (forward), 5′-GCTGCCTTGATGGACTTGAC-3′ (reverse); primer pair for mouse APP was 5′-AGACCCGTCAGGGACCAAAA-3′ (forward), 5′-TTCCACCACGTTTGTGATCTG-3′ (reverse); and mouse β-actin primer pair was 5′-CTACAATGAGCTGCGTGTGGC-3′ (forward), 5′-CAGGTCCAGACGCAGGATGGC-3′ (reverse). PCR conditions were 95°C for 20 s, 60°C for 20 s, and 72°C for 30 s for 35 cycles, with one initial heat-activating step at 95°C for 15 min.

Isolation of Detergent-Resistant Membranes. Cells were rinsed twice with PBS, scraped off plates, washed again, and lysed in MBS (25 mM MES and 150 mM NaCl, pH 6.5) containing 20 mM CHAPS (Roth, Karlsruhe, Germany) and 1% (v/v) protease inhibitor mix (Sigma). Alternatively, lysis buffer was supplemented with 1% Triton X-100 (Sigma) instead of 20 mM CHAPS. The samples were then passed four times through a 23-gauge needle and incubated at 4°C for 40 min. Then the homogenate was brought to 45% (w/v) sucrose by the addition of an equal volume of 90% (w/v) sucrose in MBS containing 20 mM CHAPS and placed at the bottom of an ultracentrifuge tube. A discontinuous sucrose gradient was formed by overlaying the homogenate successively with 30% (w/v) sucrose and 5% (w/v) sucrose (both in MBS containing protease inhibitor mix but lacking CHAPS). After centrifugation at 200,000g in a rotor (TLS-55; Beckman Coulter, Krefeld, Germany) for 2 h, nine fractions were collected from the top of the gradient. Thereafter, equal volumes (usually 20 μl) of all recovered fractions were separated by SDS-PAGE and transferred to nitrocellulose for immunoblot analysis.

Measurements of SERCA Activity. Ca^{2+}-ATPase activity was measured as described previously (Johnson et al., 2002) with some modifications. In brief, N2a cells were washed twice with PBS, collected, and resuspended in a buffer containing 20 mM Tris/HCl, pH 7.2, 100 mM KCl, 10 mM NaCl, 2 mM $MgCl_2$, 5 mM KH_2PO_4, 2 mM EGTA, and 1 mM dithiothreitol supplemented with 1% (v/v) protease inhibitor mix (Sigma). Homogenization was performed by using a loose-fitting Dounce homogenizer (15 strokes) followed by passing suspension four times through a 23-gauge needle. The homogenate was spun at 1000g at 4°C for 20 min to remove nuclei, and the supernatant was centrifuged at 15,000g at 4°C for 20 min to remove the mitochondria. The resulting supernatant was then centrifuged at 100,000g at 4°C for 40 min to pellet microsomal membranes. The microsomal fraction was resuspended in the same buffer without 2 mM EGTA to a final protein concentration of 2 to 3 μg/μl. Ca^{2+}-ATPase activity was measured using an enzyme-coupled assay, in which hydrolysis of ATP is coupled to the oxidation of NADH. Oxidation of NADH was detected by a decrease in absorption at 340 nm using a DU 800 UV/Vis spectrophotometer (Beckman Coulter). The reaction buffer contained 30 mM imidazole (Sigma), pH 6.9, 6 mM $MgCl_2$, 100 mM KCl, 20 mM NaCl, 0.4 mM EGTA, 5 mM NaN_3, 1.5 mM phosphoenolpyruvate (Sigma), 2 μM ionomycin (Sigma), 4% (v/v) pyruvate kinase/lactic dehydrogenase mix (Sigma), 0.26 mM NADH (Sigma), and 2 mM ATP (Sigma). The pH was adjusted to 7.4 before the addition of the enzymes. The reaction was started by adding 50 μl of the microsomal preparation to 950 μl of the reaction buffer.

Measurements of Steady-State Fluorescence Anisotropy. Crude membranes from N2a cells were prepared and resuspended in a buffer containing 250 mM sucrose, 3 mM imidazole, pH 7.4, and 2 mM EDTA supplemented with 1% (v/v) protease inhibitor cocktail (Sigma). The membranes were treated with various agents at 25°C with gentle agitation for 20 min followed by centrifugation at 120,000g for 1 h. The resulting pellet was washed, resuspended in the same buffer, and then fluorescence anisotropy was measured. Therefore, samples were labeled with 2 μM 1,6-diphenyl-1,3,5-hexatriene (DPH) for 30 min at 30°C. The fluorescence intensity and polarization measurements were performed on a QuantaMaster Spectrofluorometer (PTI, Toronto, ON, Canada) with excitation and emission at wavelengths of 362 (±10) and 430 nm (±10), respectively. A cutoff filter (GG395) was placed in front of the emission filter to reduce light scattering. Fluorescence intensity was measured with the excitation polarizer in the vertical position and the analyzing emission polarizer in the vertical (I_{VV}) and horizontal (I_{VH}) positions. Steady-state anisotropy, r, was calculated with following equation: $r = (I_{VV} - I_{VH}G)/(I_{VV} + 2I_{VH}G)$. The factor G was used to correct for the unequal transmission of differently polarized light.

Determination of Free Cholesterol, β-Secretase Activity Assay, and Amyloid-β ELISA. Unesterified cholesterol was quantified using the Amplex-Red cholesterol assay kit (Invitrogen) by following the manufacturer's instructions. For the determination of total cellular β-secretase activity, a fluorogenic substrate-based β-secretase activity assay kit (BioVision, Mountain View, CA) was used according to the manufacturer's instructions. Levels of secreted amyloid-β 40 and amyloid-β 42 in conditioned media were determined using quantitative colorimetric human amyloid-β 40- and amyloid-β 42-specific sandwich ELISA kits (Biosource, Camarillo, CA) following the manufacturer's instructions.

Statistical Methods. The results are expressed as mean ± S.E.M. calculated by one-way analysis of variance using SIGMA STAT software (SPSS Science, Chicago, IL). Significance between groups was further analyzed using the post hoc Tukey test. Statistical significance was accepted at a level of $p < 0.05$. The data obtained from quantitative real-time PCR analysis were applied to the relative expression software tool (Pfaffl et al., 2002) to test for significance by a randomization test (2000 randomizations).

Results

Identification of Compounds that Accelerate Amyloid-β Production. Cholesterol is a well-known factor contributing to enhanced production of amyloid-β peptides (Shobab et al., 2005). In this regard, the ability of cholesterol to alter properties of cellular membranes, which in turn affect functions of integral membrane proteins, plays an important role. The selective COX-2 inhibitor celecoxib has been shown to exhibit an inhibitory effect on SERCA, whose activity is sensitive to alterations in membrane fluidity and thus inhibited by cholesterol as well (Johnson et al., 2002; Li et al., 2004). Because celecoxib and likewise the peroxisome proliferator-activated receptor-α agonist fenofibrate were recently implied to alter APP metabolism (Gasparini et al., 2004; Kukar et al., 2005), we hypothesized that these compounds may have a mode of action similar to that of cholesterol. Therefore, several commonly used selective COX inhibitors and fibrates were investigated for their potential to

influence APP metabolism and the production of amyloid-β peptides. The compounds' effects on APP metabolism and amyloid-β secretion were examined by using N2a mouse neuroblastoma cells stably expressing the Swedish mutant form of human APP_{695} ($N2a_{Swe}$ cells) (Mullan et al., 1992). Western blot analysis revealed that of the investigated diaryl heterocycle-selective COX inhibitors and fibrates, only celecoxib, DuP-697, SC-560, fenofibrate, and clofibrate contributed to enhanced production of β-secretase-cleaved APP C-terminal fragments (CTFβ), excluding a general class effect of these compounds (Supplementary Table S1 for an overview of tested compounds). Figure 1 clearly shows that the identified fibrates and selective COX inhibitors promote the β-site cleavage of APP, the first step in the amyloidogenic cascade exerted by BACE1. Concomitant with the accumulation of APP CTFβ, we observed decreased levels of APP CTFα, which are produced by α-secretase that cleaves APP within the amyloid-β domain, thereby preventing amyloid-β production (Fig. 1, A–C). In addition, upon treatment, C-terminal APP species with higher molecular weight were observed to a higher extent (Fig. 1, asterisks). These APP species have not been well characterized, but they very likely possess the amyloid-β domain and, consequently, can give rise to the formation of amyloid-β peptides when they are directly processed by γ-secretase. To test for existing γ-secretase activity, the γ-secretase-derived product (APP CTFγ) resulting from the final cleavage of APP CTFs was analyzed on the same blot with longer exposure (Fig. 1, A–C). Quantitative differences of CTFγ could not be observed, suggesting that overall γ-secretase activity was not affected upon treatment. Furthermore, augmented levels of full-length APP were observed after treatment of cells with the examined drugs (shown for fenofibrate and celecoxib; Fig. 1, A and B).

Based on this data set, higher concentrations of amyloid-β peptides in media after treatment of cells with the examined drugs were expected. This was confirmed by immunoblot analysis after immunoprecipitation of conditioned media with the amyloid-β (1–17)-specific antibody 6E10 (Fig. 2, A and B; exemplarily shown for celecoxib and fenofibrate). Celecoxib and fenofibrate treatment provoked a massive dose-dependent increase of secreted amyloid-β peptides compared with DMSO-treated control cells. Note that the amount of amyloid-β peptides in media from control-treated cells was nearly beyond the detection limit, whereas strong signals were detected upon treatment with both fenofibrate

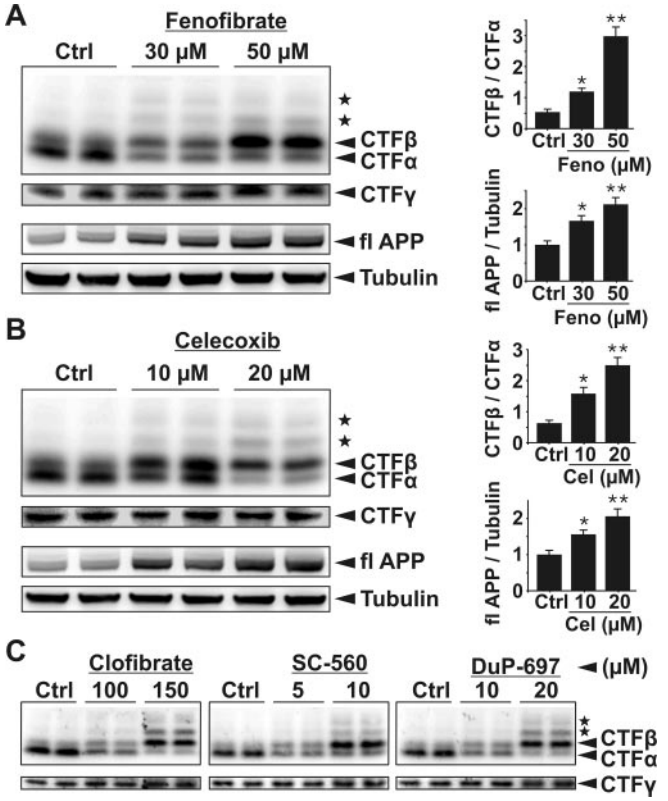

Fig. 1. Selective COX inhibitors and fibrates that promote the β-site cleavage of APP. Protein lysates of fenofibrate- (Feno, A), celecoxib- (Cel, B), clofibrate-, SC-560-, and DuP-697 (C)-treated $N2a_{Swe}$ cells (18 h) were subjected to Western blot analysis using a specific antibody directed against the C terminus of APP (A8717) to detect α-, β-, and γ-secretase-cleaved APP C-terminal fragments (CTFα, CTFβ, and CTFγ). Asterisks mark C-terminal APP species with higher molecular weight. In addition, for fenofibrate- and celecoxib-treated cells, full-length APP (fl APP) levels were analyzed by Western blot analysis. Equal protein loading was ensured by reprobing blots with tubulin-specific antibodies. Ratios of CTFβ to CTFα and fl APP to corresponding tubulin levels are depicted in the corresponding diagrams. Values are expressed as mean ± S.E.M. from three independent experiments carried out in duplicates. * and **, $p <$ 0.05 and 0.01 versus control (Ctrl), respectively, $n = 6$.

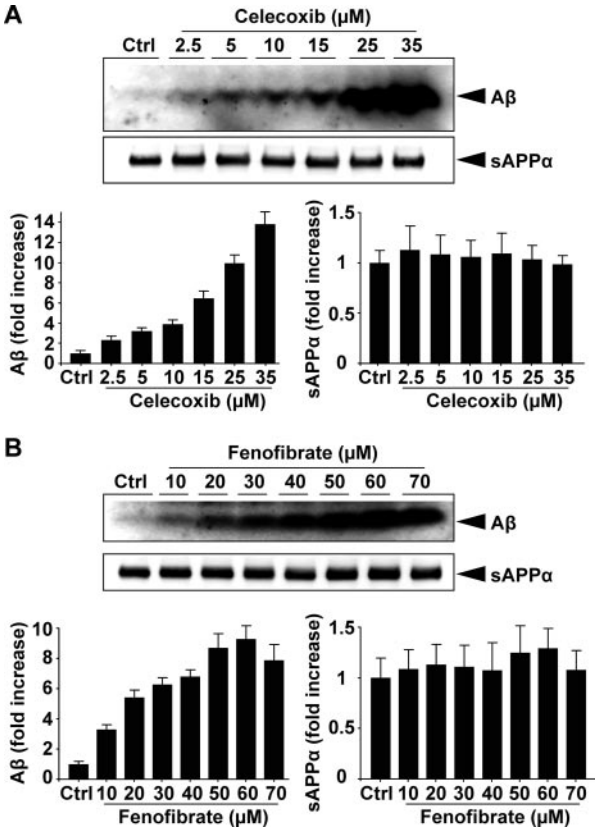

Fig. 2. Fenofibrate and celecoxib contribute to enhanced production of amyloid-β peptides. Western blot analysis of secreted sAPPα and amyloid-β peptides from celecoxib- (A) and fenofibrate (B)-treated $N2a_{Swe}$ cells (18 h) after immunoprecipitation of media with amyloid-β (1–17)-specific antibody 6E10. Amyloid-β and sAPPα levels were densitometrically analyzed and depicted in diagrams as fold increase of DMSO-treated control cells (accounted as 1). Values expressed are mean ± S.E.M. from three independent experiments. Amyloid-β levels were significantly different in all concentration groups versus control (Ctrl) and ranged from $p < 0.05$ (for 2.5 and 10 μM concentrations of celecoxib and fenofibrate, respectively) to $p < 0.001$ (for 35 μM celecoxib and 70 μM fenofibrate), $n = 3$.

and celecoxib. Furthermore, levels of sAPPα, the secreted APP derivative resulting from the α-secretase cleavage, were unchanged upon treatment, indicating that α-secretase cleavage of APP is not altered upon drug-treatment despite an observed decrease of APP CTFα levels.

Amyloid-β Promoting Agents Enhance Colocalization of APP and BACE1 in Detergent-Resistant Membrane Domains. To assess whether the accumulation of APP CTFβ and amyloid-β peptides was a result of enhanced overall BACE1 activity, steady-state BACE1 protein levels and BACE1 mRNA levels were analyzed by immunoblot and reverse transcription real-time PCR analysis, respectively. Both analyses revealed constant BACE1 levels upon treatment (Supplementary Fig. S1, A and B) and exclude higher BACE1 expression as a causal factor for enhanced amyloid-β production in fenofibrate- and celecoxib-treated cells. In addition, a commercial kit using a fluorogenic β-secretase-specific substrate was used to quantify overall BACE1 activity. This assay revealed unaltered β-secretase activity in total cell lysates from fenofibrate- and celecoxib-treated cells (Supplementary Fig. S1C). Based on these data, it was suggested that the enhanced APP processing by β-secretase could be rather caused by enhanced colocalization and consequently increased enzyme-substrate complex formation. Several reports document that the amyloidogenic processing of APP depends on DRMs (Simons et al., 1998; Cordy et al., 2003). Thus, the amyloid-β promoting agents were investigated for their potential to stabilize or recruit APP and BACE1 within these specialized membrane domains. Therefore, DRMs from celecoxib- and fenofibrate-treated N2a$_{Swe}$ cells were isolated by sucrose gradient ultracentrifugation after solubilization of cells with 20 mM CHAPS at 4°C and investigated by immunoblot analysis. Both fenofibrate and celecoxib significantly elevated the proportion of BACE1 and full-length APP in CHAPS-insoluble low buoyant density membrane fractions (Fig. 3). The detection of the DRM marker Flotillin1 served for identification of the CHAPS-extracted membrane fractions as DRMs. Besides full-length APP and BACE1, APP CTFs accumulated in DRMs upon treatment with fenofibrate and celecoxib. The treatments induced an even higher increase in APPCTFs to be localized in DRM fractions than in non-DRM fractions. Because DRMs are shown to be the platform for the γ-secretase complex as well (Vetrivel et al., 2004), the subsequent cleavage of APP CTFs by γ-secretase is very likely. In addition, DRMs were extracted also with ice-cold 1% Triton X-100 instead of 20 mM CHAPS. A similar pattern was observed with higher fractions of full-length APP, APP CTFs, and BACE1 floating with DRMs upon drug treatment (Supplementary Fig. S3).

Because integrity of DRMs is enhanced by high cholesterol concentrations (Simons and Ikonen, 1997), potential changes of cholesterol levels in fenofibrate- and celecoxib-treated N2a$_{Swe}$ cells were analyzed. However, we observed no alteration of total cellular cholesterol content upon treatment using a cholesterol oxidase enzyme-based Amplex-Red cholesterol assay kit (Supplementary Fig. S2). Thus, drug-induced higher cholesterol concentrations can be excluded as a cause for enhanced colocalization of APP and BACE1 within DRMs.

Amyloid-β-Promoting Agents Share Common Characteristics with Cholesterol. Strong evidence supports the hypothesis that cholesterol influences APP processing and promotes the formation of amyloid-β peptides by enhancing the β-site cleavage of APP (Shobab et al., 2005). In this regard, the central role of cholesterol in DRM formation is a very important aspect. Figure 3 clearly demonstrates that full-length APP, APP CTFs, BACE1, and Flotillin1 were shifted to DRMs in N2a$_{Swe}$ cells upon cholesterol treatment. Because the identified amyloid-β-promoting agents share this common characteristic with cholesterol, further similarities between these compounds and cholesterol were investigated. Therefore, N2a$_{Swe}$ cells were enriched with cholesterol, and the effects on APP processing were analyzed by immunoblot analysis. A similar pattern of steady-state APP processing was observed upon cholesterol treatment, including the accumulations of APP CTFβ, C-terminal APP fragments with higher molecular mass, and full-length APP (Fig. 4, A and B). Furthermore, the concentration of amyloid-β peptides in media from cholesterol-enriched N2a$_{Swe}$ cells was significantly increased (Fig. 4C).

Besides APP processing, further potential effects common between cholesterol and the identified amyloid-β promoting

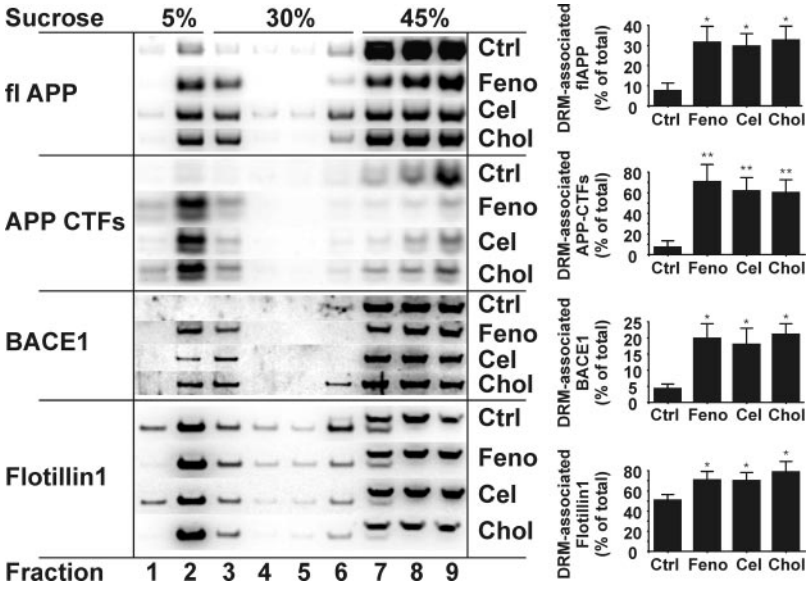

Fig. 3. Fenofibrate and celecoxib strengthen similar to cholesterol the association of APP and BACE1 with DRMs. Fenofibrate- (50 μM, Feno), celecoxib- (20 μM, Cel), and cholesterol (100 μM, Chol)-treated N2a$_{Swe}$ cells (18 h) were partially lysed with 20 mM CHAPS at 4°C and subsequently fractionated on a discontinuous sucrose density gradient by ultracentrifugation. Nine fractions were recovered from the top of the gradient and subjected to Western blot analysis with APP- and BACE1-specific antibodies. Low buoyant detergent-resistant membrane particles collected at the border between 5 and 30% sucrose (fractions 2 and 3) were identified as detergent-resistant membrane microdomains by detection of the DRM marker Flotillin1. Note that the Flotillin1 antibodies also detected an unspecific band with higher molecular weight, which was not included for quantitative analysis. Diagrams show proportions (percentage) of full-length APP (fl APP), APP C-terminal fragments (APP CTFs), BACE1, and Flotillin1 found in DRMs. Values expressed are means ± S.E.M. from three independent experiments. $*$ and $**$, $p < 0.05$ and 0.01 versus control (Ctrl), respectively, $n = 3$.

compounds were investigated. The observed increase in DRM resident APP and BACE1 upon treatment with fenofibrate, celecoxib, and cholesterol indicates changes in membrane fluidity. Hence, the fluidity of isolated cellular membranes was measured upon drug treatment by using fluorescence anisotropy with DPH as a probe. Cholesterol-enriched N2a cell membranes clearly exhibited an increase in fluorescence anisotropy, which is equivalent to a decrease in membrane fluidity (Fig. 5A). Similar to cholesterol, the amyloid-β-promoting drugs fenofibrate and celecoxib also exerted an increase in fluorescence anisotropy, indicating a rigidifying effect of the compounds on cellular membranes. The results of the fluorescence anisotropy analysis were indirectly confirmed in vitro by an enzyme-based approach by measuring the activity of SERCA, which is known to be inhibited by the cholesterol-induced ordering of membrane lipids (Li et al., 2004). As expected, cholesterol inhibited dose-dependently the Ca^{2+}-ATPase activity in a range from 5 to 100 μM (Fig. 5B). Cholesterol provoked a rather modest inhibitory action in comparison with the highly potent direct SERCA inhibitor thapsigargin that inhibited SERCA in the nanomolar range. In a similar range as cholesterol, fenofibrate and celecoxib also inhibited SERCA activity, suggesting a similar mode of action very likely by decreasing membrane fluidity. To further confirm the fluorescence anisotropy and SERCA activity measurements that were both done in cell-free assays, a cellular response to decreased membrane fluidity was examined as well. It is well acknowledged that reduced SERCA activity results in ER stress and the induction of several ER resident chaperones, including BiP/GRP78 (Li et al., 1993). Thus, we used immunoblot analysis of BiP/GRP78 expression as a parameter for a compound's potential in decreasing membrane fluidity and SERCA activity. Figure 6, C to E, shows that, similar to cholesterol, the investigated amyloid-β-promoting agents increased the expression of BiP/GRP78, confirming that the compounds lower SERCA activity like cholesterol, most likely by ordering ER membrane lipids. Thapsigargin as a direct SERCA inhibitor was used as a positive control for BiP/GRP78 induction and showed the expected increase in BiP/GRP78 levels.

Amyloid-β Promoting Drugs Do Not Interfere with the Maturation of APP. Because the induction of ER resident chaperones like BiP/GRP78 reflects a basic mechanism of cells to maintain the protein folding and maturation machinery under stress conditions, the amyloid-β-promoting drugs were investigated for their potential impact on APP maturation. Immunoblot analysis using human APP-specific antibody 6E10 that does not cross-react with endogenous mouse APP species afforded to differentiate the ectopically expressed human APP full-length species from endogenous

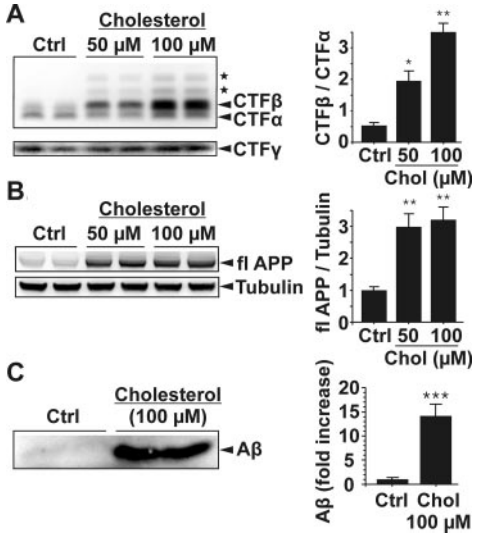

Fig. 4. Cholesterol contributes to enhanced production of amyloid-β peptides. Protein lysates from cholesterol- (Chol)-treated $N2a_{Swe}$ cells (18 h) were subjected to Western blot analysis using C-terminal APP-specific antibodies (A8717) to detect APP C-terminal fragments (CTFα, CTFβ, and CTFγ) (A) and full-length APP (fl APP, B). Asterisks mark C-terminal APP species with higher molecular weight. Depicted in diagrams are ratios of CTFβ to CTFα and fl APP to corresponding tubulin. Values expressed are means ± S.E.M. from three independent experiments done in duplicate. * and **, $p < 0.05$ and 0.01 versus control (Ctrl), respectively, $n = 6$. C, secreted amyloid-β peptides were analyzed by Western blot analysis after immunoprecipitation of conditioned media with amyloid-β (1–17)-specific antibody 6E10. In the diagram, the amyloid-β levels were depicted as the fold increase ± S.E.M. compared with levels derived from DMSO-treated control cells (considered as 1). ***, $p < 0.001$, $n = 6$.

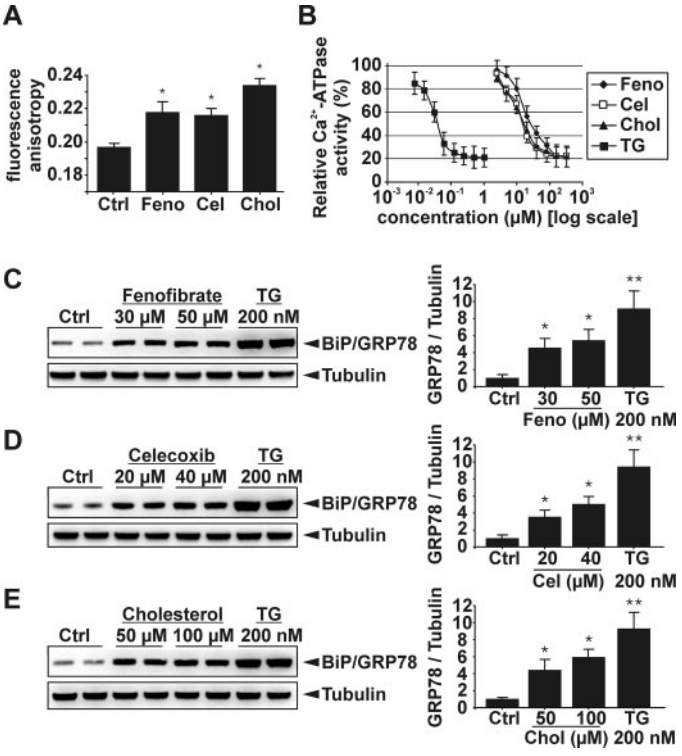

Fig. 5. Fenofibrate and celecoxib decrease membrane fluidity similar to cholesterol. A, N2a cell membranes were isolated and enriched with fenofibrate (Feno), celecoxib (Cel), and cholesterol (Chol). Thereafter, fluorescence anisotropy, which is indirectly proportional to membrane fluidity, was measured using DPH as a probe. Values are expressed as mean ± S.E.M. from three independent experiments. *, $p < 0.05$ versus control (Ctrl), $n = 3$. B, to further confirm the fluorescence anisotropy measurements, the effects of the indicated compounds on the activity of SERCA that is inhibited by a decrease of membrane fluidity, were examined as described under *Materials and Methods*. Treatment with the direct SERCA inhibitor thapsigargin (TG) served as a positive control. Values expressed are means ± S.E.M. from experiments done in triplicates. C through E, BiP/GRP78 induction as a cellular response to decreased SERCA activity was evaluated by immunoblot analysis upon treatment with the indicated compounds (18 h). The direct SERCA inhibitor thapsigargin served as a positive control. Depicted in the diagrams are ratios of BiP/GRP78 to corresponding tubulin. Values are expressed as means ± S.E.M. from three independent experiments carried out in duplicate. * and **, $p < 0.05$ and 0.01 versus control, respectively, $n = 6$.

APP and, thus, to make a clear decision about mature and immature APP bands. Figure 6 clearly shows, considering the unaltered ratios of mature to immature APP, that neither fenofibrate nor celecoxib inhibited *N*- and *O*-glycosylation of APP. Because *O*-glycosylation of APP takes place in Golgi compartments (Dunphy and Rothman, 1985), it can be assumed that APP export from ER was not disturbed and that protein folding and maturation is still maintained in the presence of the amyloid-β-promoting drugs. In contrast, upon treatment of cells with thapsigargin, the mature APP band completely disappeared, indicating an enhanced ER stress with a nearly completely disabled protein folding system. The use of tunicamycin, an inhibitor of N-linked glycosylation in the ER, served for the identification of *N*-glycosylated APP species. Note the downshift of the two APP bands because of the absence of *N*-glycans. It is interesting that the appearance of the upper APP band that probably represents *O*-glycosylated APP without *N*-glycans implies that the exit of APP from the ER to post-ER compartments is independent from N-linked glycosylation. In addition, as seen in Fig. 2, full-length APP levels increased dose-dependently after treatment with fenofibrate and celecoxib, indicating a post-transcriptional regulation of APP_{695} levels because APP_{695} was expressed ectopically.

The Amyloid-β-Promoting Effect Is Neither Cell Type-Specific nor Depends on the Swedish Mutant Form of APP. To exclude that the amyloid-β-promoting effects of the investigated drugs were limited to the $N2a_{Swe}$ cell model bearing the "Swedish" mutant form of APP that renders APP to an optimal β-secretase substrate (Grüninger-Leitch et al., 2002), the effects of the investigated drugs were examined in the parental N2a cell line as well. Therefore, N2a cells were treated with fenofibrate, celecoxib, and with the selective COX-1 inhibitor SC-560, which was found to be most potent to accelerate the amyloid-β production in $N2a_{Swe}$ cells. All drugs applied in same concentrations as in $N2a_{Swe}$ clearly provoked an increase of APP CTFβ levels in N2a cells, whereas in control-treated N2a cells, APP CTFβ was almost not detectable (Fig. 7A). Moreover, similar to the data from $N2a_{Swe}$ cells, full-length APP accumulated upon treatment. Because APP mRNA levels were unchanged (data not shown), we expected post-transcriptional mechanisms to be involved, as proposed for the $N2a_{Swe}$ cell model. Because the increase of APP CTFβ is accompanied by a nearly equivalent increase of full-length APP, and because amyloid-β levels could not be detected from endogenous source, a drug-induced stimulation of amyloid-β production cannot be defi-

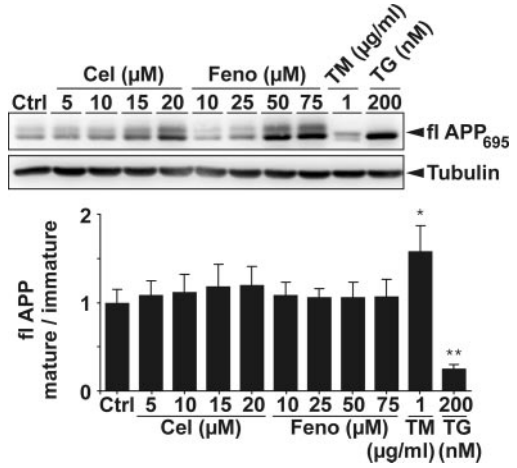

Fig. 6. Fenofibrate and celecoxib exhibit no influence on APP maturation. $N2a_{Swe}$ cells were treated with fenofibrate (Feno) and celecoxib (Cel) in different concentrations (18 h). Thereafter, protein lysates were prepared and subjected to Western blot analysis using monoclonal APP-specific antibody 6E10 to detect human full-length APP_{695}. This antibody does not cross-react with endogenous mouse APP species; thus, mature APP_{695} bands were clearly distinguishable from immature APP_{695} bands. Tunicamycin (TM) and thapsigargin (TG) served for mapping of *N*-glycosylated and *O*-glycosylated APP species, respectively. Depicted in the diagram are ratios of mature APP (*O*-glycosylated) to corresponding immature APP (non-*O*-glycosylated). Values expressed are means ± S.E.M. from three independent experiments. * and **, $p < 0.05$ and 0.01 versus control (Ctrl), respectively, $n = 3$.

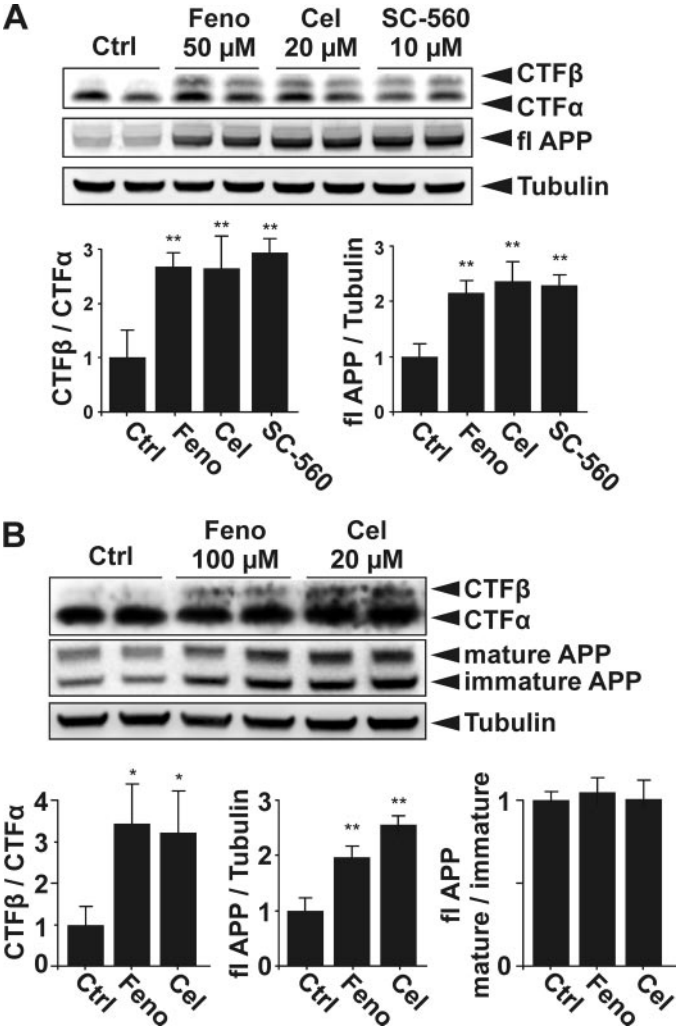

Fig. 7. Fenofibrate and celecoxib also promote the β-site cleavage of APP from endogenous APP source and in non-neuronal cells. A, protein lysates from parental N2a cells treated with fenofibrate (Feno), celecoxib (Cel), and SC-560 (18 h) were prepared and subjected to immunoblot analysis. APP-specific antibodies (A8717) were used to detect APP C-terminal fragments (CTFα and CTFβ) and full-length APP (fl APP). Equal protein loading was ensured by reprobing blots with tubulin-specific antibodies. Ratios of CTFβ to CTFα and fl APP to tubulin are depicted in the diagrams. Values are expressed as mean ± S.E.M. from three independent experiments carried out in duplicates. **, $p < 0.01$ versus control (Ctrl), $n = 6$. B, same experiments as in A but with the primary human fibroblasts cell line IMR-90. Note that in IMR-90 cells, the mature APP species were clearly distinguishable from immature APP species. Therefore, ratios of mature APP to corresponding immature APP are depicted in an additional diagram (right). * and **, $p < 0.05$ and 0.01 versus control, respectively, $n = 6$.

nitely concluded. However, with respect to the increased APP CTFβ-to-APP CTFα ratio, we infer that the drugs also stimulate the β-secretase cleavage of endogenous APP. To further extend the described effect on non-neuronal cells, we used the primary human fibroblasts cell line IMR-90, which was shown previously to be suitable for studying APP metabolism at the endogenous level (Kern et al., 2006). The experiments with this cell line mirrored the results obtained from $N2a_{Swe}$ cells and from N2a cells upon treatment with fenofibrate and celecoxib, including the accumulations of APP CTFβ and full-length APP (Fig. 7B). In addition, the accumulation of full-length APP included the immature and the mature form of APP, confirming that the drugs have no influence on APP maturation.

Celecoxib Exhibits a Dual Effect on β- and γ-Secretase in a CHO Cell Model. Celecoxib was recently identified by two independent groups as a selective γ-secretase modulator leading to enhanced production of amyloid-β 42 and decreased production of amyloid-β 40/38 without affecting total amyloid-β levels (Gasparini et al., 2004; Kukar et al., 2005). For this effect, a selective allosteric modulation of γ-secretase has been proposed as an underlying biochemical mechanism. To examine this suggested effect of celecoxib on γ-secretase, levels of secreted amyloid-β 40 and 42 peptide species in conditioned media were analyzed by colorimetric sandwich ELISA. Celecoxib-treatment of $N2a_{Swe}$ cells caused a massive increase of amyloid-β 40. To a similar extent, amyloid-β 42 levels also increased upon celecoxib treatment (Fig. 8C). These results are consistent with the Western blot analysis displayed in Fig. 2A showing a massive increase of total amyloid-β peptide levels upon celecoxib treatment. However, these data were conflicting with previously published data, which show that celecoxib-treatment of $N2a_{Swe}$ cells provokes an increase of amyloid-β 42 and, concomitantly, a decrease of amyloid-β 40 levels (Gasparini et al., 2004). To confirm our results, we performed additional experiments with a CHO cell line overexpressing the Swedish mutant form of human APP_{695} (CHO_{Swe} cells). The experiments with CHO_{Swe} cells confirmed our results obtained from the $N2a_{Swe}$ cell model and showed that celecoxib increase both APP CTFβ levels and, consequently, total amyloid-β levels (Fig. 8, A and B). In contrast to $N2a_{Swe}$ cells, celecoxib provoked a bell-shaped dose-response curve of amyloid-β levels. As shown previously, CHO cells are highly susceptible to celecoxib concentrations greater than 20 μM (Kukar et al., 2005). Thus, the decrease of amyloid-β levels with higher concentrations of celecoxib is very likely caused by the toxicity of this drug on CHO_{Swe} cells. Moreover, as seen for $N2a_{Swe}$ cells, the levels of sAPPα were unchanged (Fig. 8B). In contrast to $N2a_{Swe}$ cells, the levels of full-length APP were not elevated in CHO_{Swe} cells upon celecoxib treatment. The potential dual effect of celecoxib on γ-secretase, in addition to the promoting effect on β-secretase, was investigated in CHO_{Swe} cells. Therefore, amyloid-β 40 and 42 levels in media samples from CHO_{Swe} cells were analyzed by colorimetric sandwich ELISA. It is interesting that in this cell line, celecoxib treatment provoked a greater increase of amyloid-β 42 than amyloid-β 40 levels, suggesting that γ-secretase activity was affected by celecoxib (Fig. 8D). These results support previously published data showing that celecoxib can modulate the γ-secretase cleavage in CHO cells and that celecoxib preferentially increases amyloid-β 42 levels (Kukar et al., 2005).

Discussion

The results of the present study suggest that cholesterol and the investigated drugs display a similar mode of action,

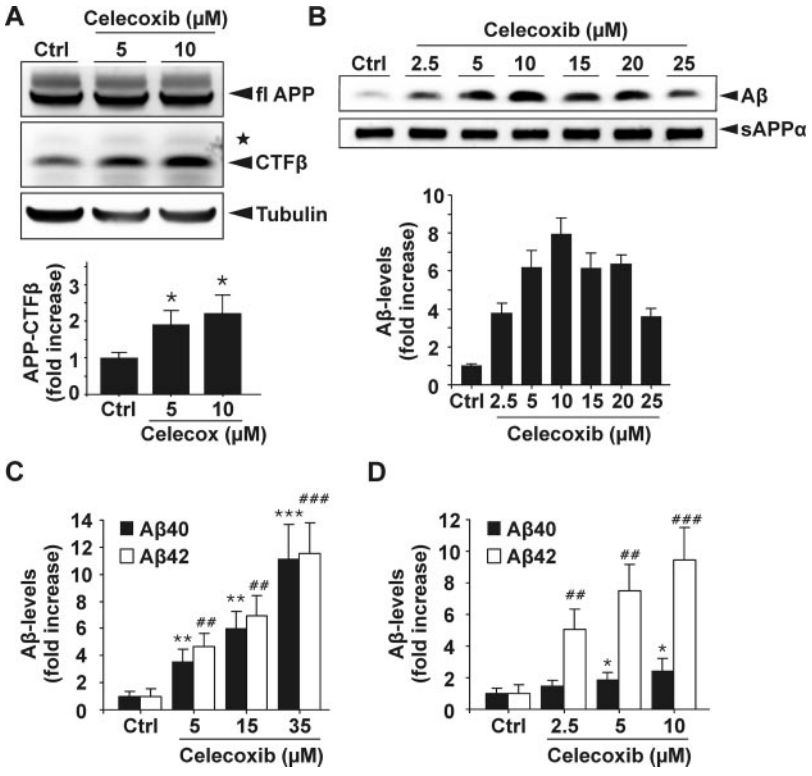

Fig. 8. Celecoxib provokes dual effect on β- and γ-secretase in CHO cells. A, protein lysates of celecoxib-treated (18 h) CHO_{Swe} cells were subjected to Western blot analysis using a specific antibody directed against the C terminus of APP (A8717) to detect full-length APP (fl APP) and β-secretase-cleaved APP CTFβ. Asterisk marks the C-terminal APP species with higher molecular weight. Equal protein loading was tested by reprobing blots with tubulin-specific antibodies. The fold increase of CTFβ levels is depicted in the corresponding diagram. Values are expressed as mean ± S.E.M. from three independent experiments carried out in duplicate. *, $p < 0.05$ versus control (Ctrl), $n = 6$. B, for the determination of secreted amyloid-β and sAPPα levels, media samples from celecoxib-treated (18 h) CHO_{Swe} cells were directly subjected to Western blot analysis using amyloid-β (1–17)-specific antibody 6E10. In the diagram, amyloid-β levels from celecoxib-treated cells were depicted as the fold increase ± S.E.M. compared with levels derived from DMSO-treated control cells (considered as 1). In all indicated concentrations, celecoxib provoked significantly elevated amyloid-β levels versus control (Ctrl), $p < 0.01$, $n = 6$. Amyloid-β 40 and 42 levels from celecoxib-treated (18 h) $N2a_{Swe}$ (C) and CHO_{Swe} cells (D) were determined by amyloid-β 40- and amyloid-β 42-specific sandwich ELISA. Values expressed are mean ± S.E.M. from two independent experiments done in duplicate. * and **, $p < 0.05$ and 0.01, respectively; ## and ###, $p < 0.01$ and 0.001 versus amyloid-β 40 and amyloid-β 42 levels, respectively, of control, $n = 4$.

leading to enhanced formation of amyloid-β peptides. This can be concluded from the fact that besides APP processing, these drugs share important biochemical effects with cholesterol concerning physical properties of biological membranes. Cholesterol drives the otherwise fluid phospholipid bilayer into a more liquid ordered state whose outcome is a decrease in membrane fluidity (Maxfield and Tabas, 2005). This effect was clearly demonstrated in a cell-free assay for cholesterol and for the amyloid-β-promoting drugs fenofibrate and celecoxib (Fig. 5A). Membrane stiffening is proposed to affect conformation and function of several integral membrane proteins (Maxfield and Tabas, 2005). This effect was demonstrated for cholesterol and for the amyloid-β-promoting drugs by their inhibitory action on SERCA, which is known to be inhibited by changes in bilayer properties. In agreement with our results, the inhibitory effects of celecoxib and cholesterol on SERCA has been shown by other groups (Johnson et al., 2002; Li et al., 2004). The reduction of SERCA activity then could have resulted in ER stress and the induction of the chaperone BiP/GRP78, because the function of SERCA is critical for maintaining the protein-folding machinery in the ER (Li et al., 1993). This aspect is well acknowledged for cholesterol and is implicated in atherosclerotic lesion instability, rupture, and thrombogenicity, whereas excessive free cholesterol induces ER stress and apoptotic cell death of macrophages (Tabas, 2002; Feng et al., 2003; Li et al., 2004). It is interesting that besides high cholesterol levels, the use of celecoxib is suggested to promote cardiovascular thromboembolic events and to increase the risk of myocardial infarction (Caldwell et al., 2006), suggesting that celecoxib might mimic cholesterol in this pathogenic mechanism by decreasing fluidity of biological membranes. The membrane effect is further supported by the high lipophilicity of the amyloid-β-promoting diaryl heterocycle cyclooxygenase inhibitors celecoxib, DuP-697, and SC-560 (C-logP = 4.4, 4.6, and 6.2, respectively) and fenofibrate (C-logP = 5.2), which expect that they reside predominantly within the membrane bilayer. In addition, valdecoxib, which exhibits no effect on amyloid-β production, has low lipophilicity (C-logP = 1.8) (Supplementary Table S1).

The effects of fenofibrate and celecoxib on biological membranes can explain their amyloid-β-promoting action when considering that the entire process of amyloidogenesis occurring in AD is associated with cellular membranes. In particular, DRMs may represent the platforms in which the amyloidogenic cascade starts exclusively (Cordy et al., 2006). Cholesterol was identified as a critical DRM component determining its stability and organization (Simons and Ikonen, 1997; Brown and London, 1998). The enhanced association of BACE1 and APP within DRMs upon cholesterol enrichment (Fig. 3) affirms this aspect. Without affecting total cholesterol levels, the amyloid-β-promoting drugs fenofibrate and celecoxib also increased the proportion of BACE1 and APP in DRMs. One plausible scenario is that APP and BACE1 are recruited and retained only in DRMs when their integrity is sufficiently stabilized by high cholesterol levels and likewise by fenofibrate and celecoxib. Therefore, it has been shown that DRMs seem to be highly dynamic structures and that cholesterol concentration can affect the DRM protein content (Simons and Toomre, 2000; Pike, 2004). This can be simply concluded from the fact that the degree of lipid order in membranes defines their resistance to mild detergents by which DRMs are extracted (Brown and London, 1998; London and Brown, 2000). The lipid-ordering and consequently the DRM-stabilizing effects of cholesterol are well-documented, and our data now provide evidence that compounds exist with similar action.

Our finding that several selective cyclooxygenase inhibitors and fibrates increase total amyloid-β levels conflicts with previous reports. Kukar et al. (2005) and Gasparini et al. (2004) have not observed elevated levels of total amyloid-β peptides upon celecoxib treatment. Instead, they found a selective increase of amyloid-β 42 levels and a simultaneous decrease of amyloid-β 38 or amyloid-β 40 peptides. We tried hard to find the basis for this obvious discrepancy and tested different incubation times, cell culture conditions, and experimental formats. These additional experiments all showed substantially the same results as presented throughout this study, and to date, we have no satisfying explanation for the observed discrepancy. One observation we made was that the basal levels of amyloid-β are varying with different culture conditions, in particular with the use of different sera, serum concentrations, and pH-buffering systems. For example, when CHO_{Swe} cells, a cell line which produces high amounts of amyloid-β peptides, were cultured with 10% active serum without HEPES buffer, the basal amyloid-β levels were strongly increased (compared with our standard condition), and the amyloid-β-promoting effect of celecoxib was strongly reduced (data not shown). These observations point to the possibility that potential saturation effects under certain culture conditions caused by the used APP overexpression cell models might have masked the effect of celecoxib on β-secretase. However, this explanation is only speculative, and we refer to our explicitly documented experimental conditions for reproduction of our results. Consistent with the Kukar study (Kukar et al., 2005), in CHO_{Swe} cells, celecoxib preferentially increased amyloid-β 42 levels, suggesting a modulation of γ-secretase activity by celecoxib in this cell model. Our data now further suggest that celecoxib, aside from the effect at the γ site, promotes the β-site cleavage of APP. Our new observation challenges an allosteric modulation of γ-secretase by celecoxib via direct interaction with the enzyme as hypothesized previously by others (Townsend and Pratico, 2005). A potential dual effect of celecoxib on β- and γ-secretase would rather indicate that there is one underlying mechanism for both effects and not two independent mechanisms. Alterations of membrane properties, as suggested by our data, would be a plausible explanation for both effects. As well described for β-secretase, the hydrophobic environment might also affect the γ-secretase activity and, thus, might define the length of an amyloid-β peptide. This is plausible in view of the unusual γ-secretase-mediated intramembrane cleavage (Kimberly and Wolfe, 2003) and the proposed physiological functions of amyloid-β 40 and 42 in cholesterol and sphingolipid homeostasis, respectively (Grimm et al., 2005).

Our data indicate that upon drug treatment, more APP molecules enter the secretory pathway. Because enhanced transcription could be excluded, post-transcriptional mechanisms have to be discussed that contribute to the additional APP amount. Post-transcriptionally altered APP levels are not uncommon because it has been shown that generally only a small fraction (~10%) of newly synthesized APP molecules enters the secretory pathway (Caswell et al., 1999). The

largest fraction of secretory proteins never passes the ER quality control and is directly degraded by ER resident proteases or by proteasomal/lysosomal systems. Accordingly, it has been shown that the fraction of APP entering the secretory pathway can be increased by the treatment of cells with different protease/proteasome inhibitors (Hare, 2001). Thus, it is likely that here the drugs provoke a suppression of catabolic APP pathways, thereby increasing the flux of APP into the secretory pathway. The drug effects on the ER membrane and the resulting induction of ER resident chaperones further highlight this possibility.

Among the compounds bearing the amyloid-β-increasing effect are the frequently used drugs fenofibrate, clofibrate, and celecoxib. These drugs are widely applied in humans for the treatment of atherosclerosis and arthritis. Our results indicate that these drugs should be used with caution because under certain conditions, they could exacerbate AD, in which amyloid-β peptides might play a central role. It should be noted that this would be only true if the concentration of drugs in the brain of humans is within the range required to induce the effects reported here. The need for a high central nervous system penetrance in humans is shown in a recent study for selective cyclooxygenase inhibitors that show brain-to-plasma ratios ranging from 2 to 3:1 (Dembo et al., 2005). This study also shows that a single normal therapeutic dose of celecoxib (200 mg) is sufficient to reach drug concentrations in the brain over several hours effectual to promote amyloid-β peptides in the present study. The fibrate drugs are usually indicated in doses ranging from 300 mg (fenofibrate) to 1500 mg (clofibrate) daily, which result in peak plasma concentrations from 28 μM (as fenofibric acid for fenofibrate) (Kubota et al., 2005) to 300 μM (as clofibric acid for clofibrate) (Matsuura et al., 1998), respectively, and thus within the concentration range used in our in vitro experiments. Nevertheless, whether clofibrate or fenofibrate can reach the brain in concentrations needed for the promotion of amyloid-β peptide production is not yet known.

In conclusion, our study provides strong evidence that several selective COX inhibitors and fibrates exhibit intrinsic physicochemical properties similar to cholesterol with respect to biological membranes that potentially contribute to the production of amyloid-β peptides. Nevertheless, whether these drugs promote amyloid-β peptide production in humans and whether their long-term clinical application could even contribute to the pathogenic cascade of Alzheimer's disease is yet unclear.

Acknowledgments

We thank Dr. Gerald Gimpl at the Institute of Biochemistry, Johannes Gutenberg-University of Mainz, for providing technical equipment and for help with the fluorescence anisotropy measurements.

References

Brown DA and London E (1998) Structure and origin of ordered lipid domains in biological membranes. *J Membr Biol* **164:**103–114.
Caldwell B, Aldington S, Weatherall M, Shirtcliffe P, and Beasley R (2006) Risk of cardiovascular events and celecoxib: a systematic review and meta-analysis. *J R Soc Med* **99:**132–140.
Caswell MD, Mok SS, Henry A, Cappai R, Klug G, Beyreuther K, Masters CL, and Small DH (1999) The amyloid beta-protein precursor of Alzheimer's disease is degraded extracellularly by a Kunitz protease inhibitor domain-sensitive trypsin-like serine protease in cultures of chick sympathetic neurons. *Eur J Biochem* **266:**509–516.
Cordy JM, Hooper NM, and Turner AJ (2006) The involvement of lipid rafts in Alzheimer's disease. *Mol Membr Biol* **23:**111–122.
Cordy JM, Hussain I, Dingwall C, Hooper NM, and Turner AJ (2003) Exclusively targeting beta-secretase to lipid rafts by GPI-anchor addition up-regulates β-site processing of the amyloid precursor protein. *Proc Natl Acad Sci U S A* **100:**11735–11740.
Dembo G, Park SB, and Kharasch ED (2005) Central nervous system concentrations of cyclooxygenase-2 inhibitors in humans. *Anesthesiology* **102:**409–415.
Dunphy WG and Rothman JE (1985) Compartmental organization of the Golgi stack. *Cell* **42:**13–21.
Feng B, Yao PM, Li Y, Devlin CM, Zhang D, Harding HP, Sweeney M, Rong JX, Kuriakose G, Fisher EA, et al. (2003) The endoplasmic reticulum is the site of cholesterol-induced cytotoxicity in macrophages. *Nat Cell Biol* **5:**781–792.
Gamerdinger M, Manthey D, and Behl C (2006) Oestrogen receptor subtype-specific repression of calpain expression and calpain enzymatic activity in neuronal cells—implications for neuroprotection against Ca-mediated excitotoxicity. *J Neurochem* **97:**57–68.
Gasparini L, Rusconi L, Xu H, del Soldato P, and Ongini E (2004) Modulation of beta-amyloid metabolism by non-steroidal anti-inflammatory drugs in neuronal cell cultures. *J Neurochem* **88:**337–348.
Grimm MO, Grimm HS, Patzold AJ, Zinser EG, Halonen R, Duering M, Tschape JA, De Strooper B, Muller U, Shen J, et al. (2005) Regulation of cholesterol and sphingomyelin metabolism by amyloid-beta and presenilin. *Nat Cell Biol* **7:**1118–1123.
Grüninger-Leitch F, Schlatter D, Kung E, Nelbock P, and Dobeli H (2002) Substrate and inhibitor profile of BACE (β-secretase) and comparison with other mammalian aspartic proteases. *J Biol Chem* **277:**4687–4693.
Hardy J and Selkoe DJ (2002) The amyloid hypothesis of Alzheimer's disease: progress and problems on the road to therapeutics. *Science* **297:**353–356.
Hare JF (2001) Protease inhibitors divert amyloid precursor protein to the secretory pathway. *Biochem Biophys Res Commun* **281:**1298–1303.
Johnson AJ, Hsu AL, Lin HP, Song X, and Chen CS (2002) The cyclo-oxygenase-2 inhibitor celecoxib perturbs intracellular calcium by inhibiting endoplasmic reticulum Ca^{2+}-ATPases: a plausible link with its anti-tumour effect and cardiovascular risks. *Biochem J* **366:**831–837.
Kern A, Roempp B, Prager K, Walter J, and Behl C (2006) Down-regulation of endogenous amyloid precursor protein processing due to cellular aging. *J Biol Chem* **281:**2405–2413.
Kimberly WT and Wolfe MS (2003) Identity and function of gamma-secretase. *J Neurosci Res* **74:**353–360.
Kubota T, Yano T, Fujisaki K, Itoh Y, and Oishi R (2005) Fenofibrate induces apoptotic injury in cultured human hepatocytes by inhibiting phosphorylation of Akt. *Apoptosis* **10:**349–358.
Kukar T, Murphy MP, Eriksen JL, Sagi SA, Weggen S, Smith TE, Ladd T, Khan MA, Kache R, Beard J, et al. (2005) Diverse compounds mimic Alzheimer disease-causing mutations by augmenting Abeta42 production. *Nat Med* **11:**545–550.
Lammich S, Kojro E, Postina R, Gilbert S, Pfeiffer R, Jasionowski M, Haass C, and Fahrenholz F (1999) Constitutive and regulated α-secretase cleavage of Alzheimer's amyloid precursor protein by a disintegrin metalloprotease. *Proc Natl Acad Sci U S A* **96:**3922–3927.
Lehmann S, Chiesa R, and Harris DA (1997) Evidence for a six-transmembrane domain structure of presenilin 1. *J Biol Chem* **272:**12047–12051.
Li WW, Alexandre S, Cao X, and Lee AS (1993) Transactivation of the grp78 promoter by Ca^{2+} depletion. A comparative analysis with A23187 and the endoplasmic reticulum Ca^{2+}-ATPase inhibitor thapsigargin. *J Biol Chem* **268:**12003–12009.
Li Y, Ge M, Ciani L, Kuriakose G, Westover EJ, Dura M, Covey DF, Freed JH, Maxfield FR, Lytton J, et al. (2004) Enrichment of endoplasmic reticulum with cholesterol inhibits sarcoplasmic-endoplasmic reticulum calcium ATPase-2b activity in parallel with increased order of membrane lipids: implications for depletion of endoplasmic reticulum calcium stores and apoptosis in cholesterol-loaded macrophages. *J Biol Chem* **279:**37030–37039.
London E and Brown DA (2000) Insolubility of lipids in triton X-100: physical origin and relationship to sphingolipid/cholesterol membrane domains (rafts). *Biochim Biophys Acta* **1508:**182–195.
Matsuura K, Hara A, Kato M, Deyashiki Y, Miyabe Y, Ishikura S, Sugiyama T, and Katagiri Y (1998) Activation of human liver 3α-hydroxysteroid dehydrogenase by clofibrate derivatives. *J Pharmacol Exp Ther* **285:**1096–1103.
Maxfield FR and Tabas I (2005) Role of cholesterol and lipid organization in disease. *Nature* **438:**612–621.
Mullan M, Crawford F, Axelman K, Houlden H, Lilius L, Winblad B, and Lannfelt L (1992) A pathogenic mutation for probable Alzheimer's disease in the APP gene at the N-terminus of beta-amyloid. *Nat Genet* **1:**345–347.
Pfaffl MW, Horgan GW, and Dempfle L (2002) Relative expression software tool (REST) for group-wise comparison and statistical analysis of relative expression results in real-time PCR. *Nucleic Acids Res* **30:**e36.
Pike LJ (2004) Lipid rafts: heterogeneity on the high seas. *Biochem J* **378:**281–292.
Rovelet-Lecrux A, Hannequin D, Raux G, Le Meur N, Laquerriere A, Vital A, Dumanchin C, Feuillette S, Brice A, Vercelletto M, et al. (2006) APP locus duplication causes autosomal dominant early-onset Alzheimer disease with cerebral amyloid angiopathy. *Nat Genet* **38:**24–26.
Shobab LA, Hsiung GY, and Feldman HH (2005) Cholesterol in Alzheimer's disease. *Lancet Neurol* **4:**841–852.
Simons K and Ikonen E (1997) Functional rafts in cell membranes. *Nature* **387:**569–572.
Simons K and Toomre D (2000) Lipid rafts and signal transduction. *Nat Rev Mol Cell Biol* **1:**31–39.
Simons M, Keller P, De Strooper B, Beyreuther K, Dotti CG, and Simons K (1998) Cholesterol depletion inhibits the generation of β-amyloid in hippocampal neurons. *Proc Natl Acad Sci U S A* **95:**6460–6464.
Tabas I (2002) Consequences of cellular cholesterol accumulation: basic concepts and physiological implications. *J Clin Invest* **110:**905–911.

Theuns J, Brouwers N, Engelborghs S, Sleegers K, Bogaerts V, Corsmit E, De Pooter T, van Duijn CM, De Deyn PP, and Van Broeckhoven C (2006) Promoter mutations that increase amyloid precursor-protein expression are associated with Alzheimer disease. *Am J Hum Genet* **78:**936–946.

Townsend KP and Pratico D (2005) Novel therapeutic opportunities for Alzheimer's disease: focus on nonsteroidal anti-inflammatory drugs. *FASEB J* **19:**1592–1601.

Vassar R, Bennett BD, Babu-Khan S, Kahn S, Mendiaz EA, Denis P, Teplow DB, Ross S, Amarante P, Loeloff R, et al. (1999) Beta-secretase cleavage of Alzheimer's amyloid precursor protein by the transmembrane aspartic protease BACE. *Science* **286:**735–741.

Vetrivel KS, Cheng H, Lin W, Sakurai T, Li T, Nukina N, Wong PC, Xu H, and Thinakaran G (2004) Association of γ-secretase with lipid rafts in post-Golgi and endosome membranes. *J Biol Chem* **279:**44945–44954.

Address correspondence to: Dr. Christian Behl, Institute for Physiological Chemistry and Pathobiochemistry, Johannes Gutenberg University Mainz, Medical School, Duesbergweg 6, 55099 Mainz, Germany. E-mail: cbehl@uni-mainz.de